Muthanna Journal of Engineering and Technology, Vol. (12), Issue (2), Year (2024)

Muthanna Journal of Engineering and Technology

Website: https://muthjet.mu.edu.iq/

Submitted 10 July, Accepted 3 Augst 2024, Published online 9 August 2024

Torsion behavior of self-compacting reinforced concrete beams produced from recycled aggregate: a numerical investigation

Ahmed Fadhil Kadhim Alfuraiji[a] and Jamal Abdulsamad Khudhair[a]

[a]Basrah University, Civil Engineering Department, Basrah health directory, Basrah, Iraq
**Corresponding author E-mail: Ahmed.alnawrs7@gmail.com*

DOI:10.52113/3/eng/mjet/2024-12-02/19-28

Abstract

In the study of reinforcement beams, the behavior of reinforcing beams under torsion is challenging. The use of numerical approaches has been extensive for this purpose, particularly in relation to experimental research, which is usually associated with costs as well as very significant difficulties. This study aims to investigate the torsional moment behavior of the properties of concrete beams, where beams are tested by subjection to torsional moments that come from the eccentricity of the applied load.

The experimental 12 self-compacted reinforcement beams models adopted for analysis in this study are tested, all beams are geometrically similar, have a rectangular cross-section with dimensions of (200x250) mm2 with 1000 mm length, within parameters considered include the recycled aggregate concrete (RCA) content, (0,25,50 and 75 %), The amount of longitudinal reinforcement and the number of stirrups.

An investigation was conducted to evaluate the convenience and efficacy of utilizing ANSYS software for modeling and performing nonlinear analysis on reinforced concrete beams subjected to pure torsion. The fracture threshold of each specimen was reached by applying a monotonic force. The identical specimens were additionally examined utilizing the methodology proposed by ACI318 to determine their torsional capabilities.

Where the application of FEM analysis allows for the assessment of cracking and fracture torques with a high level of accuracy. The torsional capacity achieved with this method was superior in precision compared to the method described in ACI318. Also, the torsional cracking morphology and the crack propagation trend were properly predicted through to the point of the crack.

Keywords: *Self-Compacting Concrete (SCC), Finite Element Method (FEM), Recycled Aggregate Concrete (RCA), Torsion, Crack, Angles of twist, SOLID65, Longitudinal bars, Stirrups,Ultimate load.*

1. Introduction

The study of torsion as a component of elasticity occurred over a century ago. Researchers have paid considerable time to analyze concrete compounds under torsion for almost 70 years [1]. The torsion problem is more difficult in both analytical and experimental contexts compared to other types of loads [2]. Performing experimental experiments to explore pure torsion problems or combined torsion and shear is a difficult assignment. In 1988, Jawad [3], proposed new formulas for determining the torsional strength and torsional stiffness of spandrel beams subjected to single or two concentrated loads. also recommended using the ACI limit design method for designing spandrel beams to resist torsion, without the need for longitudinal steel reinforcement [4].

The ANSYS 2020.R software was utilized to conduct a nonlinear finite element analysis. The chosen 3D models produced good results, as the ratios of numerical to experimental ultimate analysis exhibited consistent agreement with experimental data over the load-deflection curves [5]. However, the number of experimental specimens is limited due to the high cost of conducting experiments. Therefore, conducting finite-element analysis before to experiments is a cost-effective approach that allows for the creation of ideal specimens before proceeding with the experiments. For this reason, numerous studies have thus far aimed to study specific elements using numerical methods. Extensive research has been conducted on the nonlinear analysis of elements subjected to bending, shear, and a combination of bending and compression [6]. A limited number of studies have been conducted on torsion [7]. However, whereas bending in beams has a high level of flexibility, the behavior of concrete under torsion has similarities to that of shear in many brittle components. Therefore, it is highly important to understand the factors that have an impact on torsion. In this study, 12 experimental specimens were modeled

and analyzed using ANSYS [8] to study the parameters that affect the 3D nonlinear analysis of concrete components under torsion.

2. Modelling and nonlinear analysis of specimens

The ANSYS 2020.R software was utilized for using nonlinear finite elements for the purpose of modeling and analyzing the specimens. The specimens were modeled using Solid elements that were dimensionally similar to the laboratory specimens. The material utilized for simulating the concrete volumes, with or without reinforcing, was SOLID65. This choice was made due to its ability to accurately represent cracks under tension and crushing under compression. This element contains a total of 8 nodes, with each node having 3 degrees of freedom. Additionally, reinforcement can be incorporated in three perpendicular directions, which are determined by the volume ratio of the reinforcing steel. This property is utilized to simulate the transverse reinforcing of specimens under pure torsion.

To increase precision, the volume of each specimen in the model was partitioned into smaller components, resulting in the transverse reinforcing bar being separately modeled. The beam's cross-section is composed of smaller components that are arranged around the transverse reinforcement bars. Where the compressive strength of concrete and yield and ultimate stress of steel bars illustrated in tables (1) and (2).

The bar occupies the majority of the capacity of each component. The longitudinal bars were established using the Link8 element and connected to solid elements that represented concrete with common nodes in a continuous manner. The effects of Aggregate replacement ratio are taken into consideration through the properties of the concrete, the ANSYS program depends in its analysis on the properties of the materials and how they behave during exposure to external loads, where these properties can be predicted through the stress-strain relationship for the materials. Figure (1) shows the 3rd-dimensional model analyzed by the ANSYS 2020.R program. Implementation of the concrete material model in ANSYS 2020.R requires the following constants to be defined.

Table 1: Test result of compressive strength

RCA %	Fcu MPa at 28 days
0	42.1
25	39.4
50	36.5
75	33.2

Table 2: Test result of steel reinforcement

Bar size Ø (mm)	Test results		
	Yield stress fy (MPa)	Ultimate Strength fu (MPa)	Elongation (%)
8	468	622	11
10	490	623	12
12	505	648	13

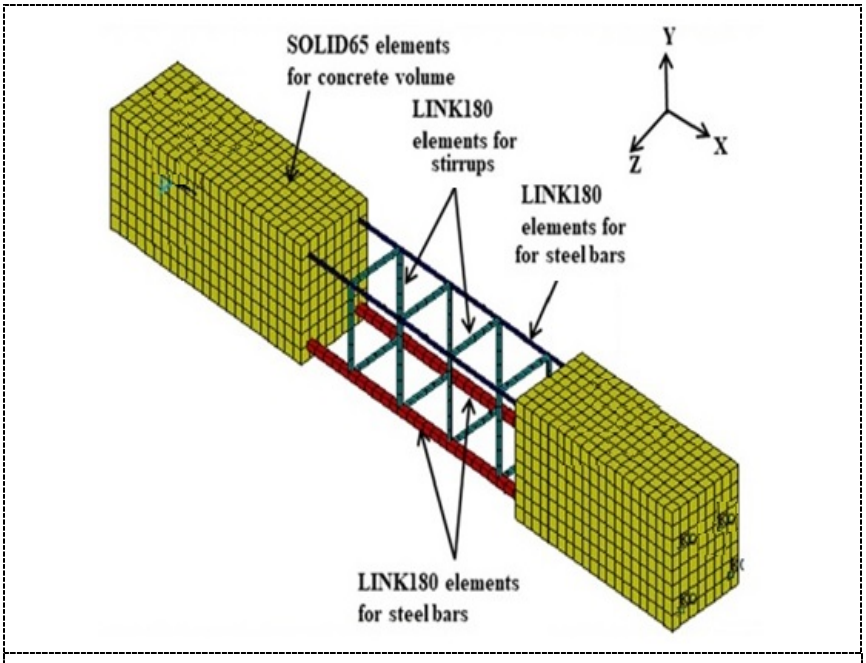

Fig. 1: Full size beam created in ANSYS.

3. Crack propagation

When the stress at a Gauss point exceeds the cracking stress along a specific direction, the element is considered to be cracked in the direction perpendicular to that specific direction. Parameter βt is very important parameter that indicates the relation between shear stresses and strains in any cracked element. This parameter is highly efficient in analyzing a specimen under torsion, as is also emphasized by others working in this field [2]. According to the results of the research conducted by [9], the value of βt for open fractures is between 0.05 and 0.25. Consequently, shear transfer on the crack surface, i.e. shear stiffness experiences a substantial decrease. Furthermore, the torsional stiffness of the concrete cross-section in an actual specimen is significantly diminished after it experiences cracking.

4. Loads and boundary conditions

In order to obtain a singular solution, it is necessary to impose displacement boundary constraints on the model. The finite element analysis findings are significantly influenced by the simulation of the applied load technique. In the experimental work of the present study, loading is applied at the end of the specimen through a stiff end winge arm, While the other end is fixed by support. Therefore, on the numerical side to ensure the actual simulation of specimens in finite element analysis, the load is applied at the ends of winge arms in such a manner that each end takes a half-applied load. The stiff end winge arms transmit the applied load evenly over the specimen end nods as shown in Figure (2).
For estimating the angle of twist caused by the applied torque, the clamp frame consists of two plates positioned on either side of the beam. The plate closest to the load side will remain stationary in all directions (U1=U2=U3=0), whereas the plate furthest from the load arm may experience a slight slip along the Y axis. The rotation of the clamp frame and beam is enabled around the Z axis, while simultaneously restricting the translational movement of the frame and base in the X and Z axes.
Failure is described in each model as the situation where the solution for a minimum load increase does not converge with the other solutions, resulting in a failure of convergence. The application following this displays a notification indicating that the models exhibit a significantly substantial distortion.

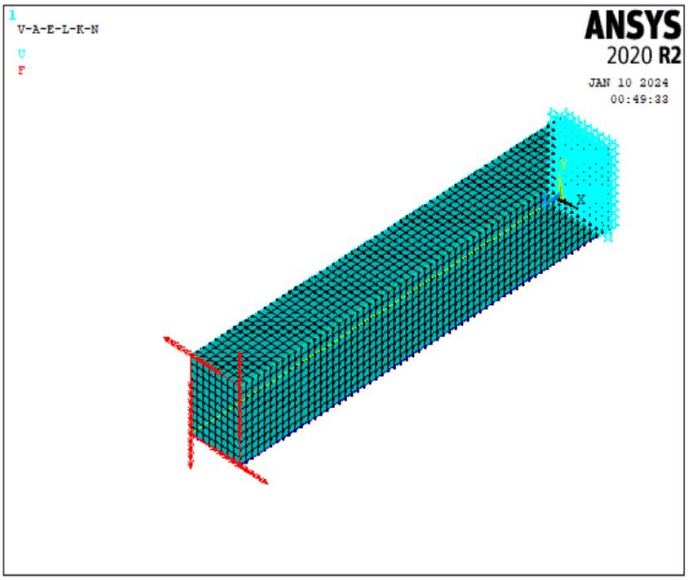

Fig. 2: Boundary conditions and loads applied on the Beam.

5. Results of finite element analysis and comparison with experimental data

The analytical findings and comparison of different outputs from the finite element models were selected to analyze the behavior of Recycled aggregate concrete (RAC) and Natural Aggregate concrete (NAC) beams. The recorded findings included the torque-twist characteristics, occurrence of cracks, maximum torque achieved, angle of twist, and distribution of torsional stresses along the greater side of the cross-section for the specimens. These results indicate a significant degree of agreement.

5.1. Experimental models

The experimental 12 self-compacted reinforcement beams models adopted for analysis in this study are tested, all beams are geometrically similar, and have a rectangular cross-section with dimensions of (200 x 250) mm^2. The parameters

considered include the RCA content, (0, 25, 50 and 75 %) and the amount of longitudinal reinforcement and stirrups as shown in Figures (3).
To generate a pure torsional moment, the load is applied by frame consisting of an I-section girder which transfers the load, applied by the testing machine, to two I-section winge arms which are fixed to the ends of the concrete beams. The testing machine applied the load centrally on the middle of the main I-section steel arm. To allow free rotation, the main steel arm connects things with the end winged arms. The load is applied pointy at the center of the main arm.

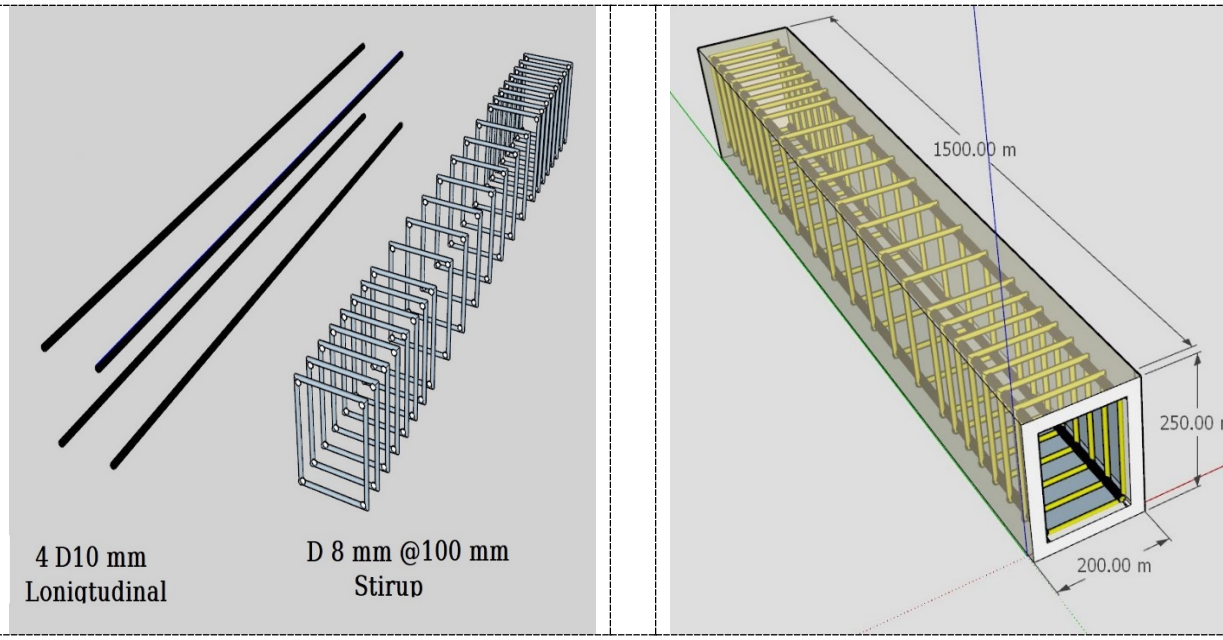

Fig. 3: Beam dimensions and distribution of reinforcement.

5.2. The cracking and ultimate torque

To facilitate comparison, the loading path is evaluated from zero to the maximum value [10]. It can be seen from the results listed in the following Table that there is a slight difference between the ultimate theoretical and experimental torques. A probable reason for the small variation between the theoretical and experimental results can be attributed to several variables: (i) the assumption of a perfect bond between the steel bars and the surrounding concrete in the theoretical model, (ii) the inclusion of the properties of concrete and the effect of RCA% through program data in the theoretical analysis, and (iii) the proficiency in testing beam specimens and the accuracy of the measuring devices utilized.
Table (3), includes the cracking and ultimate torque of experimental and theoretical test results and compares them. In the first stage of this study, for beams (group B) RS1, RSL1, and RSS1 the percentages of theoretical first cracking torques to experimental first cracking torques were: 1.12, 0.97, and 0.90, respectively. Also, the percentages of theoretical first cracking torques to experimental first cracking torques for beams (group C) RS2, RSL2, and RSS2 were: 0.95, 1.04, and 1.13, respectively, and the percentages of beams (group D) RS3, RSL3, and RSS3 were: 1.09, 1.11, and 0.94, respectively. On the other hand, for control beams (group A) S, SL, and SS were: 0.94, 1.05, and 1.08, respectively of the percentages of theoretical to experimental first cracking torque.
According to the state that the beams are no longer able to sustain additional load, which is indicated by the inability of the ANSYS program to find a solution, the ultimate torsion of the modeled beams is estimated by the state that the beams are no longer able to support the additional load.
According to the results of the experiments, the ultimate torques that were calculated utilizing the finite element model are in good accordance with the results obtained. In the second stage of the study, which dealt with solid beams (group B) with the descriptions RS1, RSL1, and RSS1, the ratios of theoretical ultimate crack torque to experimental ultimate torques were as follows: 1.12, 0.96, and 1.03, respectively. The theoretical ultimate torques to experimental ultimate torques ratios for beams in group C (RS2, RSL2, and RSS2) were 0.95, 1.09, and 1.06, respectively. Similarly, for beams in group D (RS3, RSL3, and RSS3), the ratios were 1.09, 1.13, and 1.09, respectively. However, in the case of a control beam S, the percentages of theoretical to experimental ultimate torque were 0.94, 1.11, and 1.13 for SL, and SS, respectively. Because the finite element program ANSYS 2020.R will stop immediately when the concrete element crushing or crack pathways cross element width, the numerical result curves only display the points of ultimate loads, not the failure points of loads [11].

Table 3: Experimental and theoretical test results for beams

Group	Beam Symbol	(Tcr) (EXP.) (kN.m)	(Tcr) (FEM) (kN.m)	$\frac{Tcr\ (FEM)}{Tcr\ (EXP)}$	(Tu) (EXP.) (kN.m)	(Tu) (FEM.) (kN.m)	$\frac{Tu\ (FEM)}{Tu\ (EXP)}$
	S	1,419	1.334	0.94	1,419	1.334	0.94
A	SL	1,520	1.592	1.05	6.522	7.239	1.11
	SS	1,617	1.746	1.08	7.309	8.259	1.13
	RS1	1,371	1.535	1.12	1,371	1.535	1.12
B	RSL1	1,437	1.394	0.97	6.520	6.259	0.96
	RSS1	1,511	1.36	0.9	6.969	7.178	1.03
	RS2	1,275	1.211	0.95	1,275	1.211	0.95
C	RSL2	1.287	1.338	1.04	6.392	6.967	1.09
	RSS2	1,429	1.615	1.13	6.448	6.835	1.06
	RS3	1,174	1.279	1.09	1,174	1.279	1.09
D	RSL3	1,289	1.431	1.11	5.442	6.149	1.13
	RSS3	1,318	1.298	0.94	5.871	6.399	1.09

5.3. Failure mods

In the ANSYS 2020.R program, all calculations, such as stresses and strains, are done at the points of integration of the solid elements of concrete [11]. Figure (4) shows a crack develops when the principal tensile stresses exceed the concrete tensile strength and occur perpendicular to the principal stresses.

Prenciple tensile stresses occur mostly in the xz and yz directions over the length of the beam's span (diagonal). The cracks appear perpendicular to the principal stress directions. As a result, the crack sign appears as inclined straight lines at the concrete solid elements' integration points.

These are referred to as torsional cracks. At each load step, the finite element ANSYS program will record a crack pattern [12]. Generally, the torsional cracks occur early at span ends. When the applied loads are increased, the inclined cracks spread diagonally from the span ends to the mid-span. The increasing applied loads will induce additional diagonal and sub-flexural cracks. Finally, at ultimate applied loads, the compressive cracks appeared near the supports.

The failure shapes of specimens show the onset of discrete cracks in modeled specimens will cause failure. The cracks appear to show helical forms on every side starting at the ends. This phenomenon is supposed to be the torsional cracks' spreading around the specimen sides. The first cracks in all models concentrate on the ends and show patterns along the specimen length. In all study specimens, it was noted that principal stresses and strains in the first cracked zone increased following the first cracking. Additionally, the crack-line angles were in close agreement with the experimental results, with a range of approximately 42° to 47°.

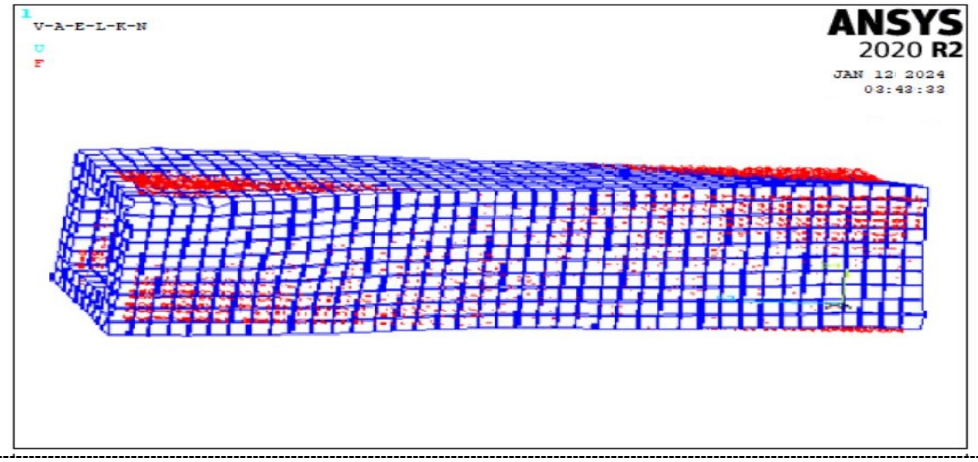

Fig. 4: Boundary typical cracks propagation beam.

Approximately, all specimens' failure modes coincided with the experimental failure modes. The ordinary concrete strength specimens (S, RS1, RS2, and RS3), and the concrete specimens with longitudinal reinforcement (SL, RSL1, RSL2, and RSL3) failed due to the development of helical cracks along the specimen length which became more impact near the ends and spalling the concrete covers around the longitudinal reinforcement near the ends as shown in typical crack propagation, and stresses intensity distribution near the longitudinal reinforcement Figure (5).

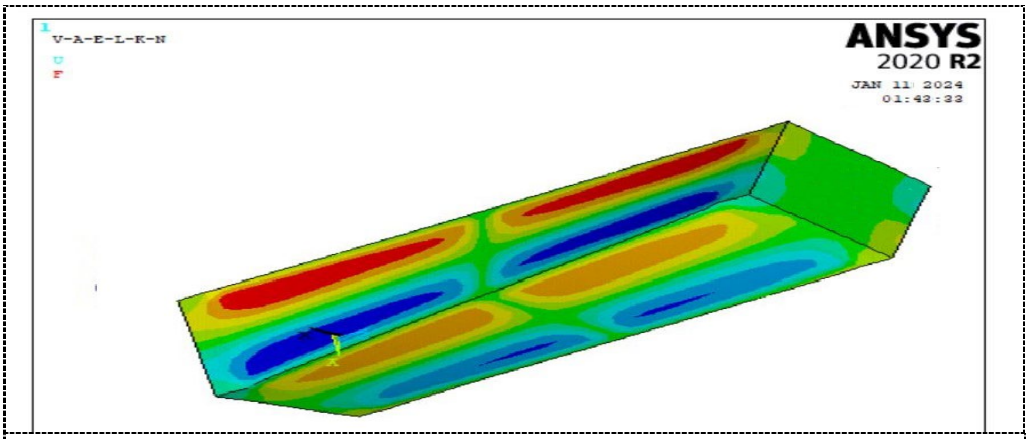

Fig. 5: Stresses intensity distribution near the longitudinal reinforcement.

According to the theoretical analysis, the specimens (SS, RSS1, RSS2, and RSS3) failed as a result of the transverse reinforcement yielding, where the stirrups near the ends reached a yielding state, Figures (6) and (7) illustrate the stresses and strains of the beams reinforcement, respectively.

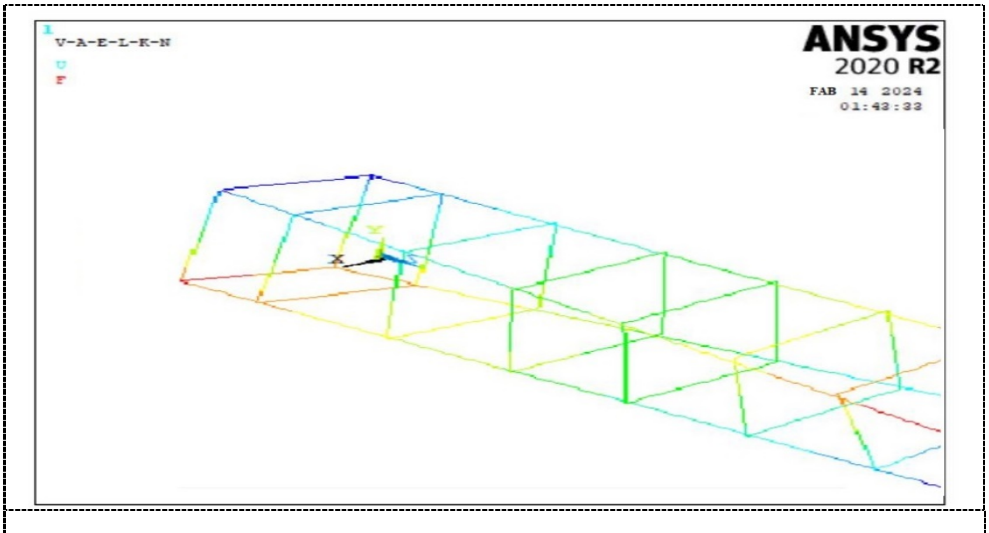

Fig. 6: Reinforcement strain.

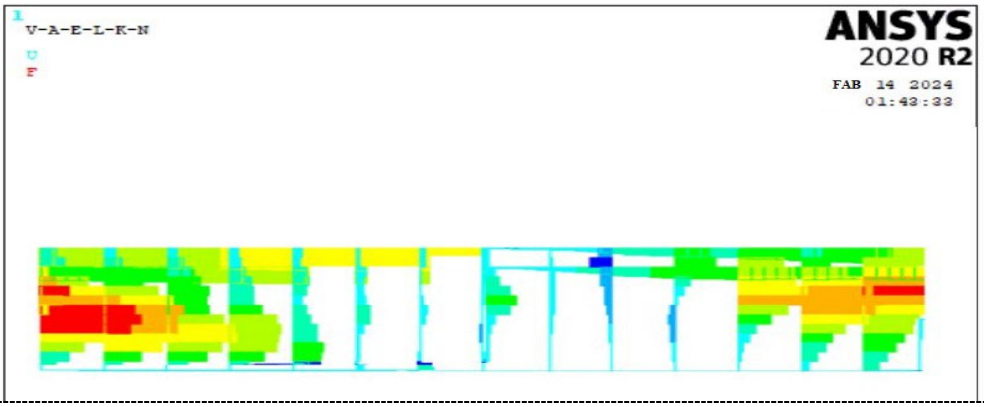

Fig. 7: Reinforcement stress distribution.

On the other hand, the specimens (RS2) failed due to concrete crushing near the ends in between the cracks as shown in Figure (8). Figure (9) shows the typical strain intensity distribution along the specimen that will propagate a helical cracked scheme during the analysis and at the ends caused the failure.

The crack in the concrete was caused by a principal tensile stress that occurred when the applied load surpassed the concrete's tensile strength. The appearance of cracks reveals the failure mode of the beams. Cracking patterns derived using finite element analysis exhibited reasonable consistency with the failure modes determined experimentally. Because of the decreased concrete stiffness, increasing the RCA ratio led to an increase in the number and width of cracks. The addition of reinforcement increases the load-carrying capacity of beams.

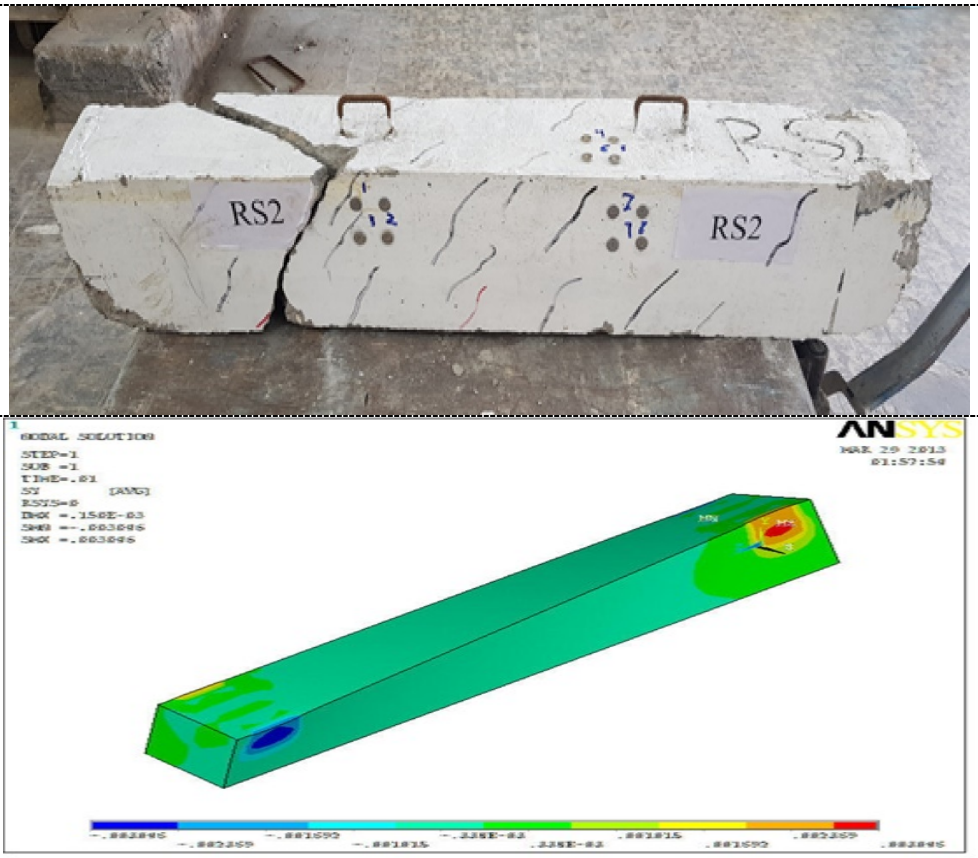

Fig. 8: Concrete crushing point.

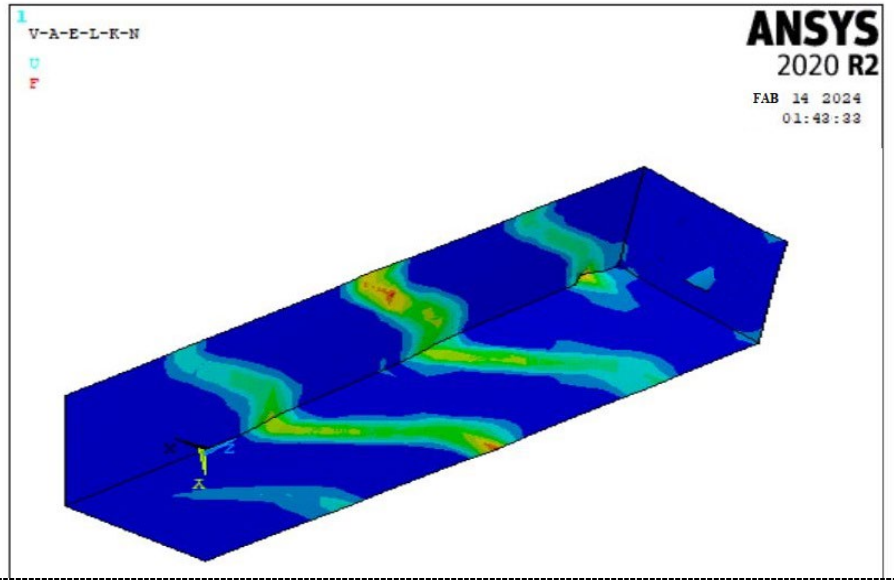

Fig. 9: Strain intensity distribution.

5.4. Failure mods

The confirmation of the finite element model is conducted by comparing the cracking torque with the angle of twists of model beams obtained from both experimental and finite element data. Tables (4) and (5) illustrate the relationship between the cracking torque and the angle of twist for all beams studied in the experimental program, conducted under monotonic loading conditions. These tables also provide the finite element solutions for both the cracking and ultimate stages.

Results of the theoretical model study, conducted using Ansys, are displayed as T-θ curves. These curves were then compared with the experimental results, as shown in Figures (10) and (11).

The torque-twist conduct shows that the finite element analysis agrees well with the experimental results across the whole range of behavior. The maximum plastic deformations occur in the midpoint of the beam's length, in accordance with the experimentally evaluated beams. The use of recycled aggregate significantly impacts the stress-strain curve of recycled

aggregate concrete. The fact that the strength of the NAC was greater than that of the RAC is certainly something that should be mentioned. The existence of an interface between old cement mortar and new cement mortar can result in a gradual development of micro-cracks at these interfaces. The stress-strain behavior and elastic modulus can be influenced by the form and surface features of recycled aggregate [13].

Table 4: Experimental and theoretical cracking torque and twist angle

Group	Beam Symbol	Experimental Value		Theoretical Value	
		Cracking Torque	Angle of Twist	Cracking Torque	Angle of Twist
	S	1,419	0.031	1.334	0.028
A	SL	1,520	0.037	1.592	0.033
	SS	1,617	0.040	1.746	0.037
	RS1	1,371	0.028	1.335	0.026
B	RSL1	1,437	0.033	1.394	0.030
	RSS1	1,511	0.037	1.46	0.035
	RS2	1,275	0.026	1.211	0.021
C	RSL2	1.287	0.029	1.338	0.026
	RSS2	1,429	0.034	1.615	0.029
	RS3	1,174	0.022	1.279	0.020
D	RSL3	1,289	0.024	1.431	0.022
	RSS3	1,318	0.031	1.298	0.028

Table 5: Experimental and theoretical ultimate torque and angle of twist for solid beams

Group	Beam Symbol	Experimental Value		Theoretical Value	
		Ultimate Torque	Angle of Twist	Ultimate Torque	Angle of Twist
	S	1,419	0.031	1.334	0.028
A	SL	6.522	1.324	7.239	1.294
	SS	7.309	2.231	8.259	2.171
	RS1	1,371	0.028	1.535	0.026
B	RSL1	6.520	1.220	6.259	1.203
	RSS1	6.969	2.078	7.178	2.005
	RS2	1,275	0.026	1.211	0.021
C	RSL2	6.392	1.112	6.967	1.092
	RSS2	6.448	1.921	6.835	1.821
	RS3	1,174	0.022	1.279	0.020
D	RSL3	5.442	1.089	6.149	1.077
	RSS3	5.871	1.851	6.399	1.671

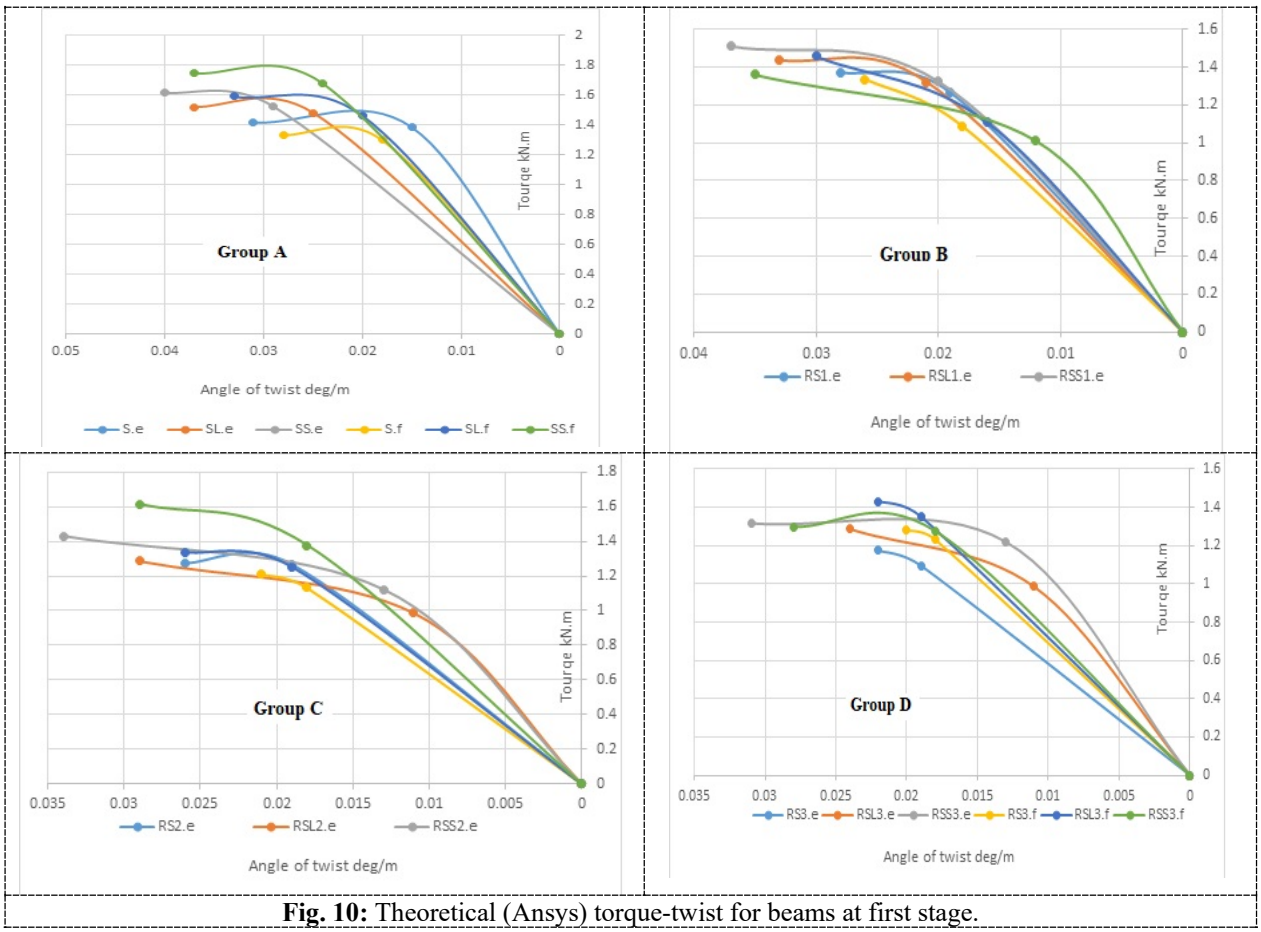

Fig. 10: Theoretical (Ansys) torque-twist for beams at first stage.

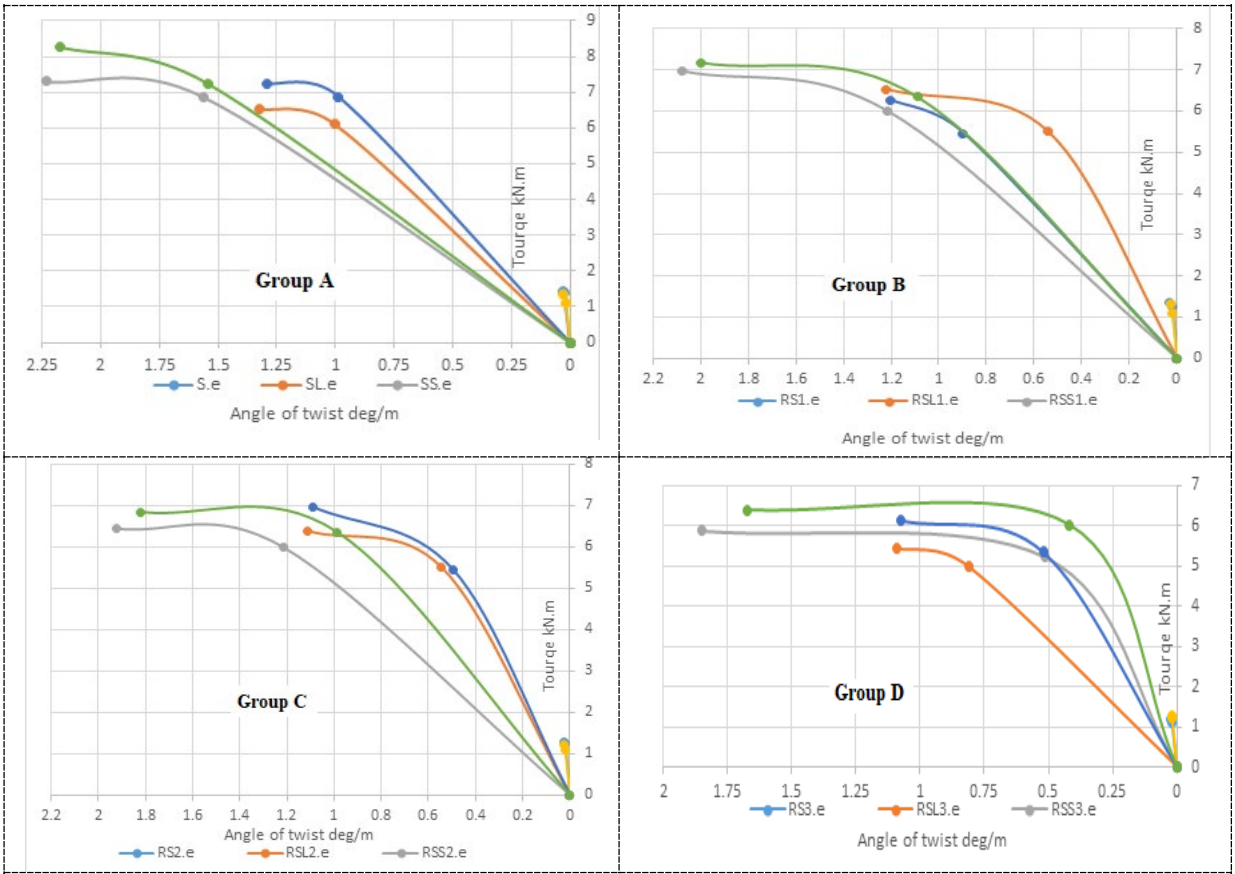

Fig. 11: Theoretical (Ansys) torque-twist behavior for beams at second stage.

6. Conclusion remarks

An investigation was conducted to evaluate the convenience and efficacy of utilizing ANSYS software for modeling and performing nonlinear analysis on reinforced concrete beams subjected to pure torsion. The research was conducted by utilizing the SOLID65 element in software to model and analyze 12 specimens that had previously been examined by other researchers. The fracture threshold of each specimen was reached by applying a monotonic force. The identical specimens were additionally examined utilizing the methodology proposed by ACI318 to determine their torsional capabilities. The primary results are as follows:

- The application of FEM analysis allows for the assessment of cracking and fracture torques with a high level of accuracy. The torsional capacity achieved with this method was superior in precision compared to the method described in ACI318.
- The torsional cracking morphology and the crack propagation trend were properly predicted through to the point of fracture.
- The torque-rotation curves produced from the experiment were consistent with those of all specimens. However, in the region after cracking occurs, where the beam's ability to resist twisting diminishes dramatically, the analysis faced difficulties in achieving convergence.
- The increase in the beam's resistance after the initial cracking comes from the presence of longitudinal reinforcing steel bars.
- The beams reinforced with transverse reinforcement demonstrated increment in both first cracking torque and ultimate torsional strength, the torque raised Some of those cracks became excessively wide, and beams fell under transversal steel given before the concrete was crushed.
- No significant difference in behavior was identified in the RCA-containing beams at the cracking stage, Where All the beams exhibited similar linear torque-rotation behavior. At the same time, RCA-containing beams show a decrease in cracking torque depending on the substitution ratio of RCA.
- There is a reasonable agreement between the experimental and the numerical result.

References

[1] Rahal K N, The behavior of reinforced concrete beams subjected to combined shear and torsion. Ph. D. thesis;1993, University of Toronto.

[2] Ameli M, and Ronagh H R. Analytical method for evaluating ultimate torque of FRP strengthened reinforced concrete beams. Journal of Composites for Construction.;2007, 11(4), pp. 1-7.
[3] Jawad, N. A. M., “Strength and Behavior of Reinforced Concrete Spandrel Beam” , M.Sc. Thesis, College of Engineering, University of Basrah,1988.
[4] ACI Committee.237 R-07, "Self-Consolidating Concrete", Reported by ACI Committee 237, PP.1-30, (2007).
[5] Malik Altaee "Structure Behavior of Reinforced Self-Compacting Concrete Slabs Containing Recycled Concrete as Course Aggregate " PhD. Thesis, College of Engineering, University of Basrah,2020.
[6] Kachlakev D, Miller T, Yim S, and Chansawat Kasidit. Finite element modeling of reinforced concrete structures strengthened with FRP laminates. Final Report for Oregon Department of Transportation Research Group;2001. Internet File.
[7] Wei R. Numerical modeling of fiber reinforced concrete beams under torsion. Final Report for Advanced Computational Modeling Center; 2005, the University of Queensland.
[8] ANSYS User's Manual ; Release 11.0, SAS IP, Inc..1454 D. Mostofinejad and S.B. Talaeitaba. / Procedia Engineering 14 (2018) 1447–1454
[9] Talaeitaba S B. Ductility enhancement of RC joints with FRP laminates, M. Sc. Thesis; 2003, Isfahan University of Technology.
[10] Naji J. H, "Non-linear finite element analysis of reinforced concrete panels and infilled frames under monotonic and cyclic loading", PhD thesis, Department of civil engineering, University of Bradford, (1989).
[11] Tavarez F. A, "Simulation of behavior of composite grid reinforced concrete beams using explicit finite element methods", M.Sc thesis, Civil Engineering, University of Wisconsin -Madison, (2001).
[12] Karayannis C. G" Analysis and Experimental Study for Steel Fiber Pullout from Cementations Matrices" Advanced Composites Letters, Vol.9, No.4, (2000).
[13] Kosmatka,S.H.,Kerkhoff, B., Panarese, W.C., MacLeod, N.F., and McGrath, R.J. “Design and Controlof Concrete Mixtures”, Seventh Edition, Cement Association of Canada, Ottawa, Ontario, Canada, 2002